12-2017

A High Quality and Quantity Hybrid Perovskite Quantum Dots ($CsPbX_3$, X= Cl, Br and I) Powders Synthesis via Ionic Displacement

Yuhang Yin
East China University of Science and Technology, China

Weiling Luan
East China University of Science and Technology, China, luan@ecust.edu.cn

Chengxi Zhang
East China University of Science and Technology, China

Fuqian Yang
University of Kentucky, fyang2@uky.edu

Repository Citation

Yin, Yuhang; Luan, Weiling; Zhang, Chengxi; and Yang, Fuqian, "A High Quality and Quantity Hybrid Perovskite Quantum Dots ($CsPbX_3$, X= Cl, Br and I) Powders Synthesis via Ionic Displacement" (2017). *Chemical and Materials Engineering Faculty Publications*. 35.
https://uknowledge.uky.edu/cme_facpub/35

A High Quality and Quantity Hybrid Perovskite Quantum Dots ($CsPbX_3$, X= Cl, Br and I) Powders Synthesis via Ionic Displacement

Notes/Citation Information

Published in *IOP Conference Series: Earth and Environmental Science*, v. 100, conference 1, 012057, p. 1-10

Digital Object Identifier (DOI)

https://doi.org/10.1088/1755-1315/100/1/012057

IOP Conference Series: Earth and Environmental Science

PAPER • **OPEN ACCESS**

A high quality and quantity hybrid perovskite quantum dots ($CsPbX_3$, X= Cl, Br and I) powders synthesis via ionic displacement

To cite this article: Yuhang Yin *et al* 2017 *IOP Conf. Ser.: Earth Environ. Sci.* **100** 012057

A high quality and quantity hybrid perovskite quantum dots ($CsPbX_3$, X= Cl, Br and I) powders synthesis via ionic displacement

Yuhang Yin[1], Weiling Luan[1, a]*, Chengxi Zhang[1], Fuqian Yang[2, b]*

[1]Key Laboratory of Pressure Systems and Safety (MOE), School of Mechanical and Power Engineering, East China University of Science and Technology, Shanghai 200237, P. R. China.

[2]Materials Program, Department of Chemical and Materials Engineering, University of Kentucky, Lexington, KY 40513, USA.

*E-mail: [a]luan@ecust.edu.cn, [b]fyang2@uky.edu

Abstract. Recently, all-inorganic perovskites $CsPbX_3$ (X= Cl, Br and I) quantum dots (QDs) have drawn great attentions because of their PL spectra tunable over the whole visible spectral region (400-700 nm) and adjustable bandgap, which revealed a promising potential on the field of photoelectronic devices, such as solar cells, LEDs and sensors. In this paper, $CsPbX_3$ QDs and hybrid QDs, CsPbClxBr3-x and CsPbBrxI3-x were synthesized via one-step and two-step methods comparably. The optical bandgaps of $CsPbCl_3$, $CsPbBr_3$, and $CsPbI_3$, were calculated as 3.08, 2.36, and 1.73eV, respectively, based on the Tauc's equation and UV absorption spectra. Ionic displacement and phase transformation occurred during the mixing process were found based on the monitoring of PL spectra and HRTEM characterization. The long-term stability, dried, high quality and two-dimensional hybrid $CsPbBrxI_{3-x}$ QDs powders could be achieved via the two-step method. Polar solution inductions were used to wash and purify the $CsPbX_3$ QDs, which help obtain of various compositions and well crystallize all-inorganic perovskites QDs powders.

1. Introduction

Organic-inorganic hybrid halide perovskite have been studied since 2009; however, only in the last five years has the vast potential of this material come to light [1, 2]. In fact, inorganic-organometallic halides with perovskite structures, such as ABX_3, have emerged as novel materials because of their unique properties, including high absorption coefficients, balanced electron/hole mobility, possible low-temperature processing, small exciton binding energies (37-75 meV), and long exciton diffusion lengths (100-1000nm) [3-8]. The cation A can be either organic or inorganic, for example, methylammonium (MA^+) or formamidinium (FA^+) for an organic cation and Cs^+ for an inorganic cation. B is a bivalent metal cation, such as Pb^{2+} or Sn^{2+}, and X is a halide, usually Cl^-, Br^-, or I^- [9, 10]. Because of these advantageous, the power conversion efficiency of solar cells which based on inorganic-organometallic halides has over 20% [11]. Although the stability of these cells have not been extensively investigated, perovskite materials are showing huge application prospects in the photoelectric field. Nowadays, many researchers are focusing on applying inorganic-organometallic halides to the display, lighting, and lasing applications. Particularly for all-inorganic halides nanocrystals (NCs) or quantum dots (QDs) ($CsPbX_3$, X=Cl, Br, I), because of the facile synthesis route, excellent luminescence efficiency, bandgap tenability, and flexible process [12-19].

Actually, QDs possess potential applications in some fields, under commercialization stage (especially in lighting and display areas). Besides, with recent breakthroughs in liquid phase synthesis, monodispersed perovskite QDs solution with high color purity and high quantum yields (QYs) can be obtained [20-23]. Compared to inorganic-organometallic halides, all-inorganic QDs materials are supposed to be with higher photo-stability, thermal stability, and chemical stability to solve the troublesome operational instability of perovskite devices. However, most of the efforts toward implementation of electroluminescent (EL) perovskite QLEDs are focused on the green-emitting $CsPbBr_3$ because of its synthesis simplicity, superior photo-electronic properties, and better matched electronic energy levels [24-28]. Other quaternary lead halide perovskite QDs such as $CsPbBr_xI_{3-x}$ or $CsPbBr_xCl_{3-x}$ are still at the stage of synthesis investigation and phosphor-related applications [29].

Recently, a huge number of articles were published on the hot injection (HI) method to synthesis the all-inorganic perovskite QDs systems. Indeed, although no surface shelling is applied, QYs as high as 90%, narrow line width and high stability make the all-inorganic perovskite family promising for both optical and optoelectronic applications, then high reaction temperature and surface passivation (shelling) are inevitable to achieve good stability and high QYs [21]. In addition, emission light covering the whole visible region (400-700 nm) is readily achieved via composition and crystal size controlling. In this paper, all-inorganic perovskite QDs with compositions of $CsPbBr_3$, $CsPbCl_3$ and $CsPbI_3$ were synthesized via hot injection. The photoluminescence (PL) of QDs were tunable by controlling the reaction temperature, especial for $CsPbBr_3$, whose size have a good linear with the temperature in 100-190 °C. However, the PL of $CsPbCl_3$ and $CsPbI_3$ were found to be tunable difficultly with the temperature. Indeed, $CsPbI_3$ was unstable extremely because its cubic structure easily transforms into an orthorhombic (yellow) structure.

In addition, perovskite QDs, whose emission light covering the whole visible region (400-700 nm) and PL tunable were synthesized via various composition. Indeed the perovskite QDs, such as $CsPbCl_xBr_{3-x}$ and $CsPbBr_xI_{3-x}$, which were synthesized via two-step are more stable than one-step synthesis. Two-step synthesis were defined as that $CsPbCl_3$, $CsPbBr_3$ and $CsPbI_3$ was obtained respectively, and then mixing them. $CsPbBr_xI_{3-x}$ which synthesized by one-step was found more unstable, and easier to be quenching. Interestingly, perovskite QDs' powders have been washed out via polar solvent induction.

2. Experimental

2.1. Chemical

Most of the chemicals used in the experiments including Cs2CO3 (99.99%), octadecene (ODE, 90%), oleic acid (OA), oleylamine (OLA, 70%), PbI2 (99.999%), PbBr2 (99.999%) and PbCl2 (99.99%) were purchased from Aladdin. Tert-butanol (^{t}BuOH) acetone and n-Hexane (>97.0%) was purchased from Lingfeng Reagent Company (Shanghai, China). All solvents and reagents were of analytical grade and directly used without further purification.

2.2 Preparation of Cs-oleate

The preparation process is similar to the previous report by L. Protesescu et al. [30] with slight different here. Typically, 195.6 mg Cs_2CO_3 was loaded into a 25 mL 3-neck flask along with 6 mL octadecene, and 1 mL OA, dried for 1 h at 120 ^{0}C, and then heated under inert argon gas to 150 ^{0}C until all Cs_2CO_3 reacted with OA.

2.3. Synthesis of $CsPbCl_xBr_{3-x}$ and $CsPbBr_xI_{3-x}$ QDs

The $CsPbCl_xBr_{3-x}$ and $CsPbBr_xI_{3-x}$ QDs could be synthesized via one-step and two-step methods according to the HI. PbX_2 was replaced by the mixing of $PbCl_2$, $PbBr_2$ and PbI_2 with the different molar ratios in process of one-step synthesis. In this study, two-step synthesis was highlighted. Firstly, $CsPbX_3$

(X=Cl, Br, I) were synthesized via the hot injection under the different temperature which mentioned above. Then, the $CsPbCl_3$ and $CsPbBr_3$, $CsPbBr_3$ and $CsPbI_3$ were mixing with the different molar ratios. The mixing solution were re-reaction for 30-60 min in the ultrasonic instrumentation. Finally, $CsPbCl_xBr_{3-x}$ and $CsPbBr_xI_{3-x}$ QDs powder could be obtained in the same washing and purify methods which mentioned above.

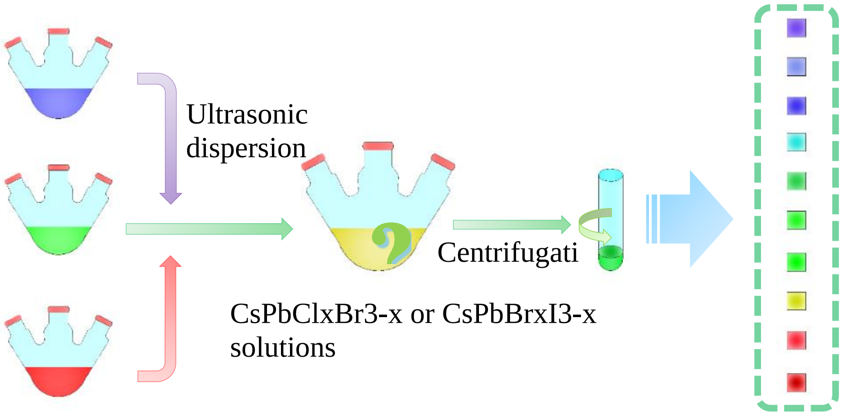

Figure 1. Scheme of two-step method to synthesize the hybrid $CsPbCl_xBr_{3-x}$ and $CsPbBr_xI_{3-x}$ QDs

3. Results and discussion

3.1. Preparation and structure of the $CsPbX_3$ QDs

$CsPbX_3$ are known to crystallize in orthorhombic, tetragonal, and cubic phase. Otherwise, perovskite QDs which were synthesis via the hot injection are cubic phase for all compounds [31-33]. In this work, the high resolution transmission electron microscope (HRTEM) (Figure.2) and the X-ray diffraction (XRD) (Figure.3) were used to show that the nanocrystals have a well-defined three-dimensional structure, which agreed well with the formation of $CsPbX_3$ QDs. Indeed, all $CsPbX_3$ QDs crystallize in the cubic phase were more stability in the room temperature which contributions from the higher surface energy in the higher reaction temperature. However, for $CsPbI_3$ NCs, this is very much a metastable state, because bulk material converts into cubic polymorph only above 315 °C. At room temperature, an exclusively PL-inactive orthorhombic phase has been reported for bulk $CsPbI_3$ (a yellow phase) [30]. Otherwise, the unclear crystallize boundary of the $CsPbI_3$ are well agreed with this point, and the $CsPbI_3$ perovskite are more or less deviated from the cubic phase which showed in the Figure.2c.

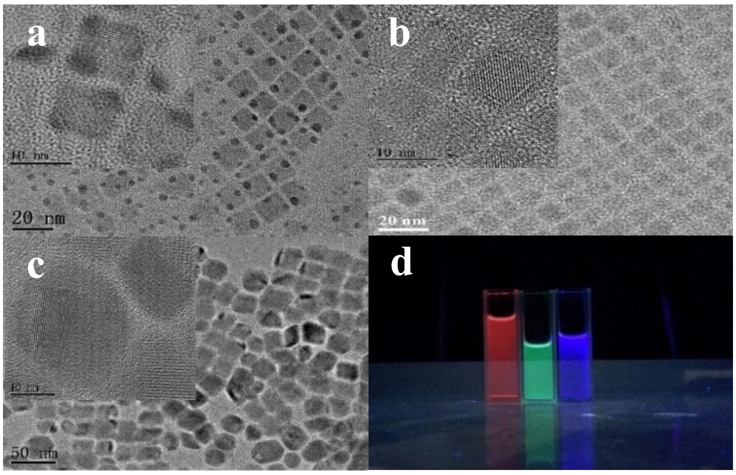

Figure 2. HRTEM images of a) $CsPbCl_3$ QDs, b) $CsPbBr_3$ QDs and c) $CsPbI_3$ QDs dispersed in n-hexane solution which were synthesized under 180 °C. d) QDs solutions images under UV light excitation.

XRD data in Fig. 3a confirm the changes of the crystal structure between the $CsPbCl_3$ QDs and $CsPbBr_3$ QDs, in which the sample with a bigger bromine amount results in a shift moved to the small angle degree [34]. Indeed, in accordance with the XRD analysis, the QDs powders (Figure. 3b) were confirmed to be well crystallized which were purified by polar solvent induction, especially for $CsPbCl_3$. But for $CsPbBr_xI_{3-x}$ which were synthesized via two-step, its diffraction peaks were disappeared which also have the fluorescence phenomenon with UV light excitation.

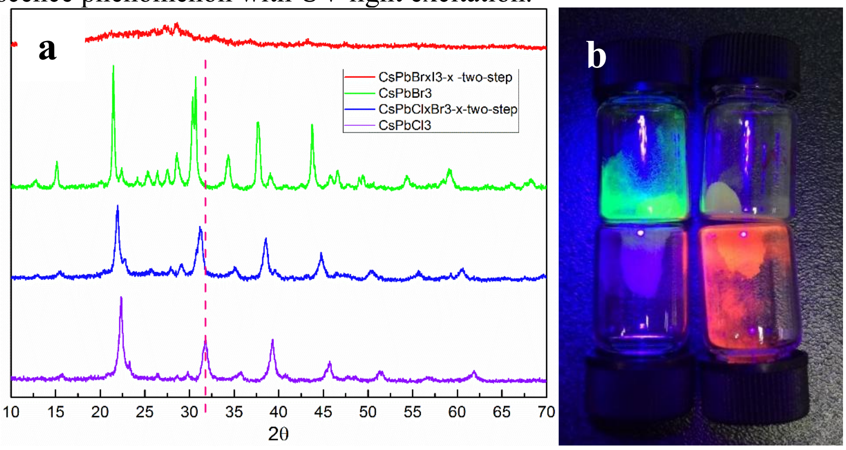

Figure 3. a) XRD patterns of $CsPbX_3$ QDs powders. b) $CsPbX_3$ QDs powders under UV light excitation.

3.2. Optical properties of the perovskite QDs

The photoluminescence (PL) spectra of colloidal perovskite QDs (Figure 4a) can be tuned over the entire visible spectral region (400-700 nm) via adjusting their composition (ratio of halides in mixed halide NCs) and reaction temperature which could change the particle size. The images of QDs in solution under UV irradiation were shown in the fig.4b. Indeed, the narrow line width of 15-40 nm indicated the excellent photoluminescence. Interestingly, with the increase of the Cl ions, the PL peak wavelength of perovskite QDs shift to ~400 nm (blue shift), instead, the PL wavelength has red shift after injecting I ions. The optical bandgaps of $CsPbX_3$ were calculated using Tauc's equation, $\alpha hv = B\ (hv - E_g)\gamma$ (E_g, energy gap; h, Planck's constants; v, frequency of incident photos; α, absorption coefficient; B constant; γ, index) [35-36]. In this case, hv was considered to be the energy (E), B was 1, α was extracted from UV-Vis absorption spectra, and γ was 1/2 due to the direct allowed transition. Based on absorption spectra, Tauc plots of $CsPbCl_3$, $CsPbBr_3$, and $CsPbI_3$ were constructed, as shown in Figure 4c, d, e, respectively. The optical bandgaps of $CsPbCl_3$, $CsPbBr_3$, and $CsPbI_3$, were calculated as 3.08, 2.36, and 1.73 eV, respectively, by finding the maximum value of E at$(\alpha E)^2 = 0$. Therefore, the optical bandgaps of $CsPbX_3$ could be adjusting via controlling the composition modulations, such as Cl, Br and I, which was very useful for improving the performance of photo-electronic devices based on all-inorganic perovskite.

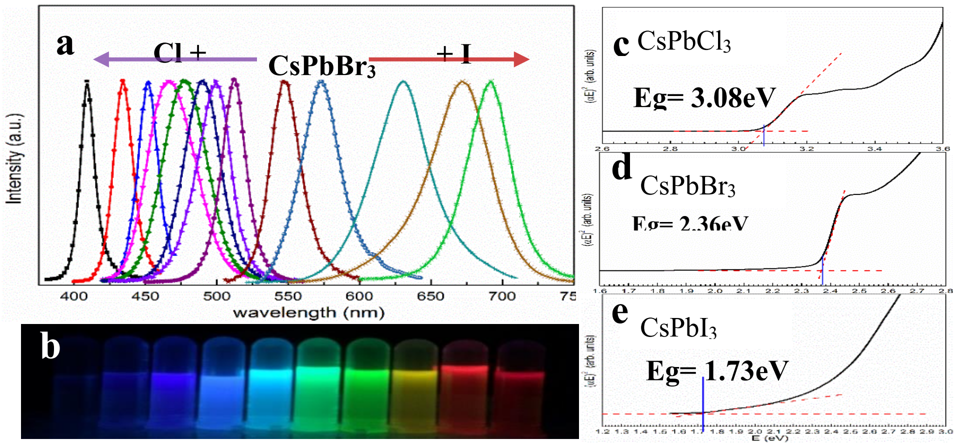

Figure 4. a) PL spectra of the $CsPbX_3$ (X=Cl, Br and I) QDs b) $CsPbX_3$ QDs images dispersed in hexane solution under UV light excitation. Tauc's plots of c) $CsPbCl_3$ QDs, d) $CsPbBr_3$ QDs and e) $CsPbI_3$ QDs. Bandgap of $CsPbCl_3$ QDs, $CsPbBr_3$ QDs and $CsPbI_3$ QDs were 3.08 eV, 2.36 eV and 1.73 eV, respectively.

3.3. Preparation and structure of the mixing $CsPbX_3$ (X = Cl、Br、I)

Although the PL spectra peaks of all-organic perovskite QDs could be tuned via adjusting the synthesis temperature (Figure. 4a), controlling the composition modulations of $CsPbX_3$ was more practical than changing the reaction temperature. Fig. 5a showed the PL spectra of $CsPbCl_xBr_{3-x}$ and $CsPbBr_xI_{3-x}$ which have the different molar ratios for Cl、Br and I ions. $CsPbCl_3$、$CsPbBr_3$ and $CsPbI_3$ were synthesized in the 3-neck flask under 180 °C, respectively, then they were mixed in the different molar ratios to obtain the hybrid $CsPbX_3$ QDs (Figure.1). The PL spectra of hybrid QDs were tunable in the whole visible region (400-700 nm) just via adjusting the hybrid molar ratios. Otherwise, the hybrid $CsPbX_3$ QDs solutions showed the different brightly color with UV light excitation (Figure.5c).

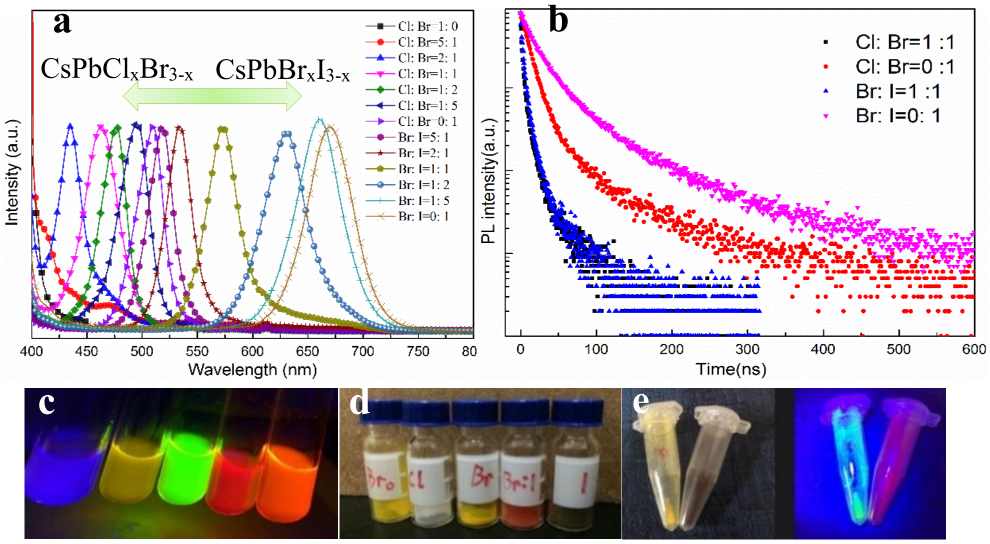

Figure 5. a) The PL spectra of hybrid $CsPbX_3$ QDs which were synthesized via two-step method. b) Time-resolved PL spectra of $CsPbX_3$ QDs solutions (hexane). c) Hybrid $CsPbX_3$ QDs solutions images under the UV light excitation. d) The dried powders of $CsPbX_3$ QDs which were washing out by the polar solutions induction. d) The powders of $CsPbBr_3$ and $CsPbI_3$ QDs under light and UV light excitation, respectively.

To gain more optical properties of hybrid $CsPbX_3$ QDs, time-resolved PL spectra were measured, as shown in fig. 5b. In accordance with the time-resolve spectra analysis, the average PL lifetime of the $CsPbBr_3$ and $CsPbI_3$ QDs were longer than the hybrid $CsPbX_3$ QDs, such as $CsPbCl_xBr_{3-x}$ and $CsPbBr_xI_{3-x}$. To achieve a better understanding of this phenomenon, the PL decay can be described by biexponential fitting, $A(t) = A_1\,exp\left(\frac{-t}{\tau_1}\right) + A_2 exp(\frac{-t}{\tau_2})$ ($A_1, A_2, \tau_1,\ \tau_2$ are the fitting coefficient, and $\tau_1,\ \tau_2$ were defined as PL lifetime of quantum dots), giving a short-lived PL lifetime (τ_1) and long-lived PL lifetime (τ_2).

Table 1. Biexponential fitting of the time-resolved PL lifetime, short-lived lifetime and long-lived lifetime were obtained.

	Short-lived lifetime (τ_1)/ns	**Long-lived lifetime (τ_2)/ns**
$CsPbCl_xBr_{3-x}$	4.88	30.56
$CsPbBr_3$	39.30	163.77
$CsPbBr_xI_{3-x}$	5.09	27.10
$CsPbI_3$	54.19	166.05

The biexponential decay behavior strongly suggested that two different species are involved in the emission. According to the study of surface-related emission in highly luminescent CdSe QDs [37], the short-lived PL lifetime is attributed to the recombination of initially generated excitons upon light absorption, while the long-lived PL lifetime component may correlate to the exciton recombination with the involvement of surface states due to the stable exciton at room temperature. Indeed, PL lifetime of $CsPbX_3$ QDs could be changed via adjusting the composition and surface state of QDs. Therefore, OA-OLA acted as surface ligands during synthesis reaction makes the QDs come to surface passivation which contributed to the higher long-lived PL lifetime, about 160 ns for $CsPbBr_3$ and $CsPbI_3$. This well agreed with the amount of reports that the PL lifetime could be increased via surface ligands modification of the QDs.

However, the long-lived PL lifetime of hybrid perovskite QDs, such as $CsPbCl_xBr_{3-x}$ and $CsPbBr_xI_{3-x}$, which were synthesized by two-step method, had decreased greatly, about 30 ns. On the one hand, the surface state of hybrid $CsPbX_3$ QDs was destroyed in the process of mixing that maybe lead to the great decreasing in the long-lived lifetime. In the typically case, the surface ligands, OA-OLA were destroyed, which increased the density of defect states on the surface of hybrid QDs. On the other hand, when comes to the mixing of the $CsPbCl_3$ and $CsPbBr_3$, because of the PL spectra peak of $CsPbCl_3$ QDs was shorter than $CsPbBr_3$, so the $CsPbCl_3$ QDs could be regarded as donor, and $CsPbBr_3$ QDs was acceptor. So resonance energy transfer (RET) might happened between the donor and the acceptor, which might result in the quenching of donor. Indeed, this phenomenon of quenching could contribute to the decreasing of the lifetime [38]. Otherwise, this case would happened in the mixing solution of $CsPbBr_3$ and $CsPbI_3$.

As the same moment, The PL spectra have confirmed that the mixing process was not just simple dispersion, but some reactions happened among the hybrid $CsPbX_3$ QDs at room temperature. Otherwise, resonance energy transfer (RET) was not concerned to be the factor that resulted in the great decreasing for the hybrid QDs. What’s more, the PL spectra just have one peak for the hybrid $CsPbX_3$ QDs after fully mixing, which showed that substitution reaction happened in the mixing process at the room temperature. As for mixing of $CsPbCl_3$ and $CsPbI_3$, there was displacements between Cl ions and Br ions in the perovskite cubic lattices. That reaction might damage the initial surface states of $CsPbBr_3$ and $CsPbI_3$, so the density of defect states of hybrid $CsPbX_3$ would increase during the substitution reaction, which led to the great reduced in the long-lived PL lifetime.

Surely, the high synthesis temperature which contributed to high surface energy and the OA-OLA surface ligands which could reduce the density of defect states, that made a difference in keeping the cubic phase for $CsPbX_3$ at the room temperature which were synthesized by one-step. Indeed the crystal structure of cubic phase and the ionic radius of Cl and Br were very similar, although there was a little difference in surface energy for $CsPbCl_3$ and $CsPbBr_3$ QDs, the surface energy of QDs was tend to be homogeneous and stability during the mixing process. Due to that, displacement reaction would happen for the Cl ionic and I ionic in the different cubic lattices under the slow and mild reaction conditions, which resulted in lots of defect states for the hybrid QDs. The same case was suit for the mixing process of the $CsPbBr_3$ and $CsPbI_3$ QDs.

Interestingly, although the OA-OLA surface ligands of $CsPbX_3$ QDs could make a difference for keeping QDs stability, actually the surface ligands have double side effect on photo-electronic devices. On the one hand, a large number of ligands are needed to provide sufficient surface passivation, which can get rid of surface defects, inducing high ink stability [39, 40]. On the other hand, excessive ligands will form an insulating layer because oleylamine and oleic acid organics used in the synthesis of $CsPbX_3$ QDs all have very poor electric conductivity, and then block charge injection [41, 42]. Besides, $CsPbX_3$ QDs were difficult to be washed out and purified from nonpolar solutions via centrifugation due to excessive ligands which led to low productivity. Therefore, in order to obtain the pure $CsPbX_3$ QDs powders, appropriate polar solutions (acetone) was induced to reprecipitation process. Indeed, the OA-OLA surface ligands could be removed, then dried QDs powders could obtain via centrifugation and dried about 1 hour at the 60 ºC. Surprisingly, in accordance with the XRD analysis, the QDs powders (fig. 5b) were confirmed to be well crystallized which were purified by polar solvent induction, especially for $CsPbCl_3$. But for $CsPbBr_xI_{3-x}$ which were synthesized via two-step, its diffraction peaks were disappeared which also have the fluorescence phenomenon with UV light excitation.

To achieve a better understanding of this phenomenon, the high resolution transmission electron microscope (HRTEM) was used to character the crystal structure of $CsPbBr_xI_{3-x}$ and $CsPbCl_xBr_{3-x}$. Fig. 6a shown that the crystal structure of $CsPbCl_xBr_{3-x}$ which were synthesized by two-step was still cubic phase, which confirmed that there was just substitution reaction happened during the mixing process and reprecipitation. On the contrary, for the $CsPbBr_xI_{3-x}$ QDs, Figure.6b showed that the crystal structure was not cubic, but a kind of two-dimensional sheet material. This confirmed that expect for substitution reaction happened in the mixing process, the cubic phase of hybrid $CsPbX_3$ transformed into other phase (orthorhombic phase). Indeed, it kept the fluorescence phenomenon with UV light excitation that was different from $CsPbI_3$ QDs. On the one hand, it was known that the $CsPbX_3$ had three types phase, orthorhombic, tetragonal, and cubic phase. And the lattice energy of cubic phase was higher than orthorhombic phase (17kJ/mol higher than orthorhombic phase in the cubic phase for $CsPbI_3$ QDs), so it was tend to change into the orthorhombic with the temperature decreasing [30, 43]. However, during the synthesis process, high reaction temperature induced the high surface energy which contributed to the $CsPbX_3$ QDs keep cubic phase at room temperature. Indeed, for $CsPbI_3$ QDs, if it were to keep cubic phase at room temperature, it needed to gain the higher surface that induced to higher reaction temperature, up to 305 ºC. Therefore, because of the density of surface defects increasing which decreased the surface energy of $CsPbI_3$ QDs, so the cubic phase transformed into the orthorhombic with the substitution reaction. But $CsPbCl_3$ QDs had very cubic phase stability, so the phase transformation didn't happen. On the other hand, amount of reports showed that the sum of halide/Pb atomic ratios in $CsPbX_3$ was greater than 3 in all $CsPbX_3$ compounds, otherwise, the proper chemical passivation of the Br-rich surface was benefit to increase PL quantum yield [13, 44]. So while Br ions were induced into the hybrid $CsPbBr_xI_{3-x}$ QDs, although the cubic phase transformed into orthorhombic phase, the hybrid $CsPbX_3$ QDs still have the fluorescence phenomenon. Indeed, two-dimensional QDs was more stable than three-dimensional materials (cubic phase). Therefore, the purified QDs powders could be obtained by the polar solutions induction and keep long-terms stability after drying at 60 ºC for 1 hour.

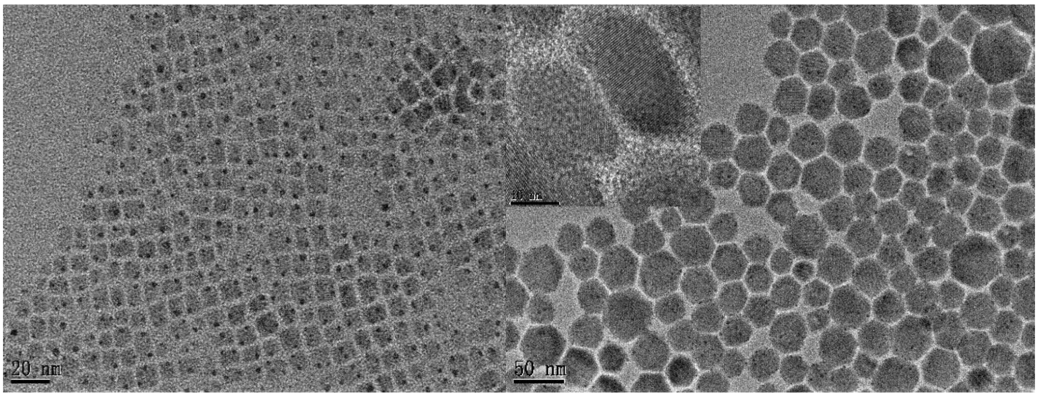

Figure 6. HRTEM images of a) $CsPbCl_xBr_{3-x}$ QDs and b) $CsPbBr_xI_{3-x}$ QDs which were synthesized via two-step method.

4. Conclusions

In this paper, all-organic perovskite quantum dots $CsPbX_3$ (X= Cl, Br and I), $CsPbCl_xBr_{3-x}$ and $CsPbBr_xI_{3-x}$ were synthesized via one-step and two-step methods, respectively, under the different reaction temperature range in 80-210 °C. The PL spectra peaks of $CsPbX_3$ QDs were tunable over the entire visible spectral region (400-700 nm) via adjusting the synthesis temperature and composition molecules. Thus, the optical bandgaps of $CsPbCl_3$, $CsPbBr_3$, and $CsPbI_3$, were calculated as 3.08, 2.36, and 1.73 eV, respectively, by finding the maximum value of E at $(\alpha E)^2 = 0$ in the Tauc's plots. Surprisingly, the PL spectra peaks were easier to be tuned via controlling the composition molecules than changing the temperature. So two-step method was used to synthesize the hybrid $CsPbX_3$ with the different PL spectra peaks via changing the mixing molar ratios. Interestingly, the average PL lifetime of $CsPbX_3$ QDs were great longer than hybrid $CsPbX_3$ which were synthesized by the two-step method. From the time-resolve PL spectra fitting and the changes of the PL spectra peaks during the mixing process, it was found that substitution reaction between the Cl ions and Br ions or the Br ions and I ions led to the density of surface defects increasing which contributed to the long-lived PL lifetime (~30 ns) were shorter than $CsPbX_3$ QDs (~160 ns) synthesized by one-step, extremely. Otherwise, during the mixing process, for the hybrid $CsPbCl_xBr_{3-x}$ QDs, some of the Cl ions in the cubic lattices of the $CsPbCl_3$ QDs were displaced by the Br ions, while some of the Br ions in the cubic lattices of the $CsPbBr_3$ QDs were displaced by the Cl ions respectively. But the phase transformations didn't happen during this process. On the contrary, for the hybrid $CsPbBr_xI_{3-x}$, ionic displacement happened between the Br ions and I ions during the mixing process, indeed, because of the low-stability for $CsPbI_3$ QDs at room temperature, the cubic crystal structure was transformed into orthorhombic phase that was a kind of two-dimensional perovskite material. Compared to cubic phase, the two-dimensional hybrid $CsPbBr_xI_{3-x}$ QDs was more stable under circumstance of the polar solutions and moisture. So all-inorganic perovskite powders could be obtained without fluorescence quenching via polar solutions reprecipitation and drying process.

References

[1] Y. Zhang, H. Wang, Z. Zhang, Y. Zhang and C. Sun, *Physical Chemistry Chemical Physics*, 2017, **19**, 1920–1926.

[2] M. a. Green, a. Ho-Baillie and H. J. Snaith, *Nature Photonics*, 2014, **8**, 506–514.

[3] Z. Tan, R. S. Moghaddam, M. L. Lai, P. Docampo, R. Higler, F. Deschler, M. Price, A. Sadhanala, L. M. Pazos, D. Credgington, F. Hanusch, T. Bein, H. J. Snaith and R. H. Friend, *Nature Nanotechnology*, 2014, **9**, 687–692.

[4] G. Li, Z. Tan, D. Di, M. L. Lai, L. Jiang, J. H. Lim, R. H. Friend and N. C. Greenham, Nano Lett, 2015, 15, 2640-2644.

[5] Y. Kim, H. Cho, J. H. Heo, T. Kim, N. Myoung, C. Lee, S. H. Im and T. Lee, *Adv. Mater*, 2015, **27**, 1248–1254.

[6] X. Li, D. Yu, F. Cao, Y. Gu, Y. Wei, Y. Wu, J. Song and H. Zeng, *Adv. Funct. Mater*, 2016, **26**, 5903–5912.

[7] J. Song, L. Xu, J. Li, J. Xue, Y. Dong and X. Li, *Adv. Mater*, 2016, **28**, 4861–4869.

[8] Y. Dong, Y. Gu, Y. Zou, J. Song, L. Xu, J. Li and J. Xue, *Small*, 2016, **12**, 5622–5632.

[9] J. Lee, D. Kim, H. Kim, S. Seo, S. M. Cho and N. Park, *Adv. Energy Mater*, 2015, **5**, 1501310.

[10] G. E. Eperon, S. D. Stranks, C. Menelaou, M. B. Johnston, L. M. Herz and H. J. Snaith, *Energy Environ. Sci.*, 2014, **7**, 982–988.

[11] S. D. Stranks and H. J. Snaith, *Nat. Nanotechnol.*, 2015, **10**, 391–402.

[12] Y. Ling, Z. Yuan, Y. Tian, X. Wang, J. C. Wang, Y. Xin and K. Hanson, *Adv. Mater,* 2016, **28**, 305–311.

[13] F. Zhang, H. Zhong, C. Chen, X. Wu, X. Hu and H. Huang, *ACS. Nano*., 2015, **3**, 4533–4542.

[14] S. Yakunin, L. Protesescu, F. Krieg, M. I. Bodnarchuk, G. Nedelcu, M. Humer, G. De Luca, M. Fiebig, W. Heiss and M. V Kovalenko, *Nature Communications*, 2015, **6**, 1–8.

[15] Y. Chih, J. Wang, R. Yang, C. Liu, Y. Chang, Y. Fu, W. Lai, P. Chen, T. Wen, Y. Huang and C. Tsao, *Adv. Mater*, 2016, **28**, 8687–8694.

[16] V. K. Ravi, G. B. Markad and A. Nag, *ACS. Energy Lett.*, **1**, 665-671.

[17] J. Li, S. G. R. Bade, X. Shan and Z. Yu, *Adv. Mater*, 2015, **27**, 5196–5202.

[18] H. Huang, F. Zhao, L. Liu, F. Zhang, X. Wu, L. Shi, B. Zou, Q. Pei and H. Zhong, *ACS Appl. Mater. Interfaces*, 2015, **7**, 28128−28133.

[19] H. Lin, L. Zhu, H. Huang, C. J. Reckmeier, C. Liang, A. L. Rogach and W. C. H. Choy, *Nanoscale*, 2016, **8**, 19846–19852.

[20] A. Swarnkar, R. Chulliyil, V. K. Ravi, M. Irfanullah, A. Chowdhury and A. Nag, *Angew.Chem. Int. Ed.*, 2015, **54**,15424 –15428

[21] X. Li, Y. Wu, S. Zhang, B. Cai, Y. Gu, J. Song and H. Zeng, *Adv. Funct. Mater*, 2016, **26**, 2435–2445.

[22] J. De Roo, M. Iba, P. Geiregat, G. Nedelcu, W. Walravens, J. Maes, J. C. Martins, I. Van Driessche, M. V Kovalenko and Z. Hens, *Acs. Nano*, 2016, **10**, 2071-2081.

[23] H. C. Yoon, H. Kang, S. Lee, J. H. Oh, H. Yang and Y. R. Do, *ACS Appl. Mater*. Interfaces, 2016, **8**, 18189−18200.

[24] S. Kumar, J. Jagielski, S. Yakunin, P. Rice, Y. Chiu, M. Wang, G. Nedelcu, Y. Kim, S. Lin, E. J. G. Santos, M. V Kovalenko and C. Shih, *ACS Nano*, 2016, **10**, 9720−9729.

[25] N. Yantara, S. Bhaumik, F. Yan, D. Sabba, H. A. Dewi, N. Mathews, P. P. Boix, H. V. Demir and S. Mhaisalkar, *J. Phys. Chem. Lett,* 2015, **6**, 4360−4364.

[26] X. Zhang, H. Lin, H. Huang, C. Reckmeier, Y. Zhang, W. C. H. Choy and A. L. Rogach, *Nano Lett.,* 2016, **16**, 1415−1420.

[27] X. Zhang, B. Xu, J. Zhang, Y. Gao, Y. Zheng and K. Wang, *Adv. Funct. Mater.,* 2016, **26**, 4595–4600.

[28] H. Huang, H. Lin, S. V Kershaw, A. S. Susha, W. C. H. Choy and A. L. Rogach, *J. Phys. Chem. Lett.*, 2016, **7**, 4398−4404.

[29] C. Huang, S. Huang and M. M. Liu, *Organic Electronics,* 2017, **44**, 6-10.

[30] L. Protesescu, S. Yakunin, M. I. Bodnarchuk, F. Krieg, R. Caputo, C. H. Hendon, R. X. Yang, A. Walsh and M. V Kovalenko, *Nano Lett*., 2015, **15**, 3692−3696.

[31] D. Zhang, S. W. Eaton, Y. Yu, L. Dou and P. Yang, *J. Am. Chem. Soc.,* 2015, **137**, 9230−9233.

[32] D. M. Trots and S. V Myagkota, *Journal of Physics and Chemistry of Solids*, 2008, **69**, 2520–2526.

[33] C. C. Stoumpos, C. D. Malliakas and M. G. Kanatzidis, *Inorganic Chemistry*, 2013, **52**, 9019–9038.

[34] J. Song, J. Li, X. Li, L. Xu, Y. Dong and H. Zeng, *Adv. Mater.,* 2015, **27**, 7162–7167.

[35] F. A. Mir, S. u. Rehman, K. Asokan, S. H. Khan, G. M. Bhat, *Appl. Phys. A*, 2014, **116**, 1017-1023.

[36] F. A. Mir, G. M. Bhat, K. Asokan, K. M. Batoo and J. A. Banday, *J Mater Sci: Mater Electron,* 2014, **25**, 431–437.
[37] X. Wang, L. Qu, J. Zhang, X. Peng and M. Xiao, *Nano Lett.*, 2003, **8**, 1103-1106.
[38] J. R. Lakowicz, *Principles of Fluorescence Spectroscopy Joseph R . Lakowicz*,
[39] Y. Chen, W. Su and S. Liou, *J. Mater. Chem.*, 2008, **18**, 675–682.
[40] A. H. Ip, S. M. Thon, S. Hoogland, O. Voznyy, D. Zhitomirsky, R. Debnath, L. Levina, L. R. Rollny, G. H. Carey, A. Fischer, K. W. Kemp, J. Labelle, K. W. Chou, A. Amassian, I. J. Kramer, Z. Ning and E. H. Sargent, *Nat. Nanotechnol.*, 2012, **7**, 577-582.
[41] M. V. Kovalenko, M. Scheele, D. V. Talapin, *Science*, 2009, **324**, 1417-1420.
[42] J. Tang, K. W. Kemp, S. Hoogland, K. S. Jeong, H. Liu, L. Levina, M. Furukawa, X. Wang, R. Debnath, D. Cha, K. W. Chou, A. Fischer, A. Amassian, J. B. Asbury and E. H. Sargent, *Nature Materials*, 2011, **10**, 765–771.
[43] H. S. Jung and N. G. Park, *Small*, 2015, **11**, 10–25.
[44] Q. Van Le, M. Park, W. Sohn, H. W. Jang and S. Y. Kim, *Adv. Electron, Mater.*, 2017, **3**, 1600448.